Structural Engineering and Mechanics, *Vol. 68, No. 1 (2018) 121-130*
DOI: https://doi.org/10.12989/sem.2018.68.1.121

Optimum shape and length of laterally loaded piles

Luigi Fenu*[1], Bruno Briseghella[2a] and Giuseppe Carlo Marano[2a]

[1]Department of Civil & Environment Engineering and Architecture, University of Cagliari, Via Marengo 2, 09123 Cagliari, Italy
[2]College of Civil Engineering, Fuzhou University, No. 2 Xue Yuan Road, University Town, Fuzhou 350108 - Fujian, China

(Received May 31, 2017, Revised August 4, 2018, Accepted August 7, 2018)

Abstract. This study deals with optimum geometry design of laterally loaded piles in a Winkler's medium through the Fully Stressed Design (FSD) method. A numerical algorithm distributing the mass by means of the FSD method and updating the moment by finite elements is implemented. The FSD method is implemented here using a simple procedure to optimise the beam length using an approach based on the calculus of variations. For this aim two conditions are imposed, one transversality condition at the bottom end, and a one sided constraint for moment and mass distribution in the lower part of the beam. With this approach we derive a simple condition to optimise the beam length. Some examples referred to different fields are reported. In particular, the case of laterally loaded piles in Geotechnics is faced.

Keywords: Winkler's soil model; fully stressed beam; FSD method; optimum length

1. Introduction

In Geotechnics and in Foundation Structure Design, laterally loaded piles are currently used, for instance, as foundation of retaining walls, harbour embankments, off-shore wharfs, and bridge abutments. These are members subjected to prevalent bending with often negligible axial loads, see for instance Poulos and Davis (1980) and Bowles (1996). Therefore, although currently called "laterally loaded piles", they behave as beams, because they are laterally loaded at the top and only restrained by the surrounding soil.

As in the case of other members subjected to bending, their design can be optimised through suitably shaping them (Haftka and Gürdal, 1993). Additionally, since they are constrained by the surrounding soil only (that is without any point constraint), their length can also be optimised. In laterally loaded piles it is frequently just checked to be sufficient, but not optimised.

Optimisation of laterally loaded piles has been faced by some authors. Fenu and Serra (1995) and Fenu (2005) optimised the pile shape by first defining the differential equation of the laterally loaded pile, and by then solving Euler's equations to find the shape of the pile minimizing its horizontal top displacement. Fenu and Madama (2006) optimised laterally loaded R/C bored piles made of two segments (with different diameters) in order to minimise their top displacement. Piles optimal shapes in integral abutment bridges has been investigated by Briseghella *et al.* (2017), by taking into account the importance of suitably designing the piles of integral abutment bridges, see for instance Zordan and Briseghella (2007), Briseghella and Zordan (2007), Zordan *et al.* (2011), Zordan *et al.* (2011), Kim *et al.* (2013), Kim *et al.* (2014).

Through implementing a genetic algorithm, Nakhaee and Johari (2013) optimised the lateral load bearing capacity of laterally loaded piles by varying diameter, length and mechanical properties. Eicher *et al.* (2002) carried out a parametric study of an offshore concrete pile, analysed by finite elements, subjected to combined loading conditions. A parametric study of the lateral behaviour of cast in drilled hole piles was carried out by Baki *et al.* (2016). A parametric analysis to study the effect of pile dimension and soil properties on the nonlinear dynamic response of pile subjected to lateral sinusoidal load at the pile head was conducted by Mehndiratta *et al.* (2014).

Based on a number of experimental data achieved from the literature, Gandomi and Alavi (2012) used neural networks to design laterally loaded piles and reliably predict their performances. Performance functions for laterally loaded single concrete piles in homogeneous clays were defined by Imancli *et al.* (2009).

In this paper, the soil surrounding the pile has been modelled as a Winkler's medium (Winkler 1867, Baguelin *et al.* 1977). Of course, a soil-pile interaction more adherent to reality could be accounted for (David and Forth 2011, Ashour and Norris 2000, Boulanger *et al.* 1999, Kim and Jeong 2011, Kavitha *et al.* 2016), McGann and Arduino (2011), as well as a better model of the soil behavior (McGann and Arduino 2011, McGann *et al.* 2011, Chik *et al.* 2008, Ahmadi and Ahmari 2009, Juirnarongrit and Ashford 2004, Broms 1964, Kok and Huat 2008, Krishnamoorthy and Sharma 2008, Phanikanth *et al.* 2010, Wakai *et al.* 1999, Yang and Jeremic 2002). Since the Winkler's soil model allows to achieve sufficiently well approximated results (Poulos and Davis 1988, Reese and Desai 1977, Brown and Shie 1990, Han and Frost 2000), this simplified model has been adopted.

*Corresponding author, Researcher
E-mail: lfenu@unica.it
[a]Professor

ISSN: 1225-4568 (Print), 1598-6217 (Online)

Optimization of the mass distribution along the pile has been obtained through a well-known optimality criterion, the Fully Stressed Design (FSD) method (see for instance Bartholomew and Morris 1976, Haftka and Gürdal 1993, Patnaik and Hopkins 1998).

Structural optimization has been common for a long time in mechanical and aeronautical engineering. In civil engineering, it is being progressively adopted both for buildings and for bridges (Briseghella *et al.* 2013, 2014, 2015, 2016, Fiore *et al.* 2016, Greco *et al.* 2016, Greco and Marano 2016, Lucchini *et al.* 2014, Marano *et al.* 2014, Marano and Greco 2011, Marano *et al.* 2013, Quaranta *et al.* 2014, Zordan *et al.* 2010). The FSD method, herein adopted, holds at the minimum weight design for statically determinate structures (Haftka and Gürdal 1993). Moreover, also in most cases of statically indeterminate structures made of a single material, a fully stressed design near the optimum is obtained. For this reason, the FSD method has been extensively used, for instance, in the aerospace industry (Haftka and Gürdal 1993).

In this paper laterally loaded piles without any axial load are considered. Therefore, since by a mechanical point of view they behave as beams, in the following we refer to "beams" when describing their mechanical behaviour and the procedure to optimize their shape and length. Besides in Geotechnics, the optimization method described in the following can be applied also in other fields, for instance to optimise steel fasteners embedded in wood, in concrete or in other materials, through defining the coefficient of subgrade reaction of the Winkler's medium as a function of the elastic modulus of the material surrounding the fastener. Nevertheless, when explicitly referring to the Geotechnics field, we will use the noun "piles", as usual in Geotechnics (Poulos and Davis 1980, Bowles 1996).

To optimise the beam shape, the FSD method was herein coupled with the Finite Element (FE) method. After performing the structural analysis of the beam by finite elements, the mass was redistributed through the FSD method. Structural analysis and mass distribution were then still updated, and this procedure iteratively performed until convergence was attained.

A similar problem was studied by Fenu and Serra (1995) and Fenu (2005), but, in both cases, the subgrade reaction on the beam occurred only along a strip with unit width. The optimum solution was found by using the calculus of variations and integrating by finite differences the system of differential equations obtained from Euler's conditions.

In this paper, the soil reaction was instead assumed to be proportional to the beam width, as it usually happens in real problems. This means that, by varying the cross-section along the beam, the reaction of the elastic soil varies as well, thus obtaining a model more representative of many real cases in a number of engineering applications. Of course, for soil reaction varying with the beam width, the problem becomes more complex. Nevertheless, a simple design solution can be achieved by using the FSD method. Finally, variational calculus was successfully used to identify the optimum length of fully stressed beams in a Winkler's medium. This allowed to define some their peculiar characteristics.

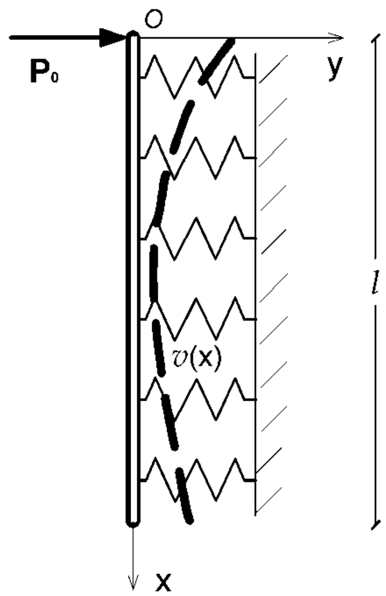

Fig. 1 Model of the beam in the Winkler's medium

2. Model of the beam in the Winkler's medium

The beam with variable cross-sectional area $A(x)$ is subjected to a soil reaction proportional to its width $D(x)$. If circular sections are used, $D(x)$ is the pile diameter (external diameter in case of circular hollow sections). The reference system (O,x,y) has its origin at the top of the beam, whose axis coincides with the abscissa axis (Fig. 1). $\mathbf{P}_0$ is the horizontal force acting at the top, V the volume of the beam, l its length, k_h the coefficient of subgrade reaction of the Winkler's medium. Since rotations at the top are free, the moment $M_0=M(x=0)$ is zero. The soil reaction varies along the beam as

$$k(x) = k_h D(x) \tag{1}$$

In many problems k_h is constant along the beam length. This is the case of steel fasteners embedded in homogeneous concrete or in wood. In Geotechnics, in 1948 Palmer and Thompson (1948) provided the general expression $k_h = k_L\ (z/L)^n$, where k_L is the value of k_h at the pile tip $(z=L)$, and $n \geq 0$ is an empirical index, usually assumed to be 0 for overconsolidated clays (k_h = const) and 1 for soft clays and granular soils (where k_h linearly varies with depth). In overconsolidated clays, k_h can be considered as practically constant along the pile for considerable depths, and assumed to be 67 c_u per unit pile width (Davisson 1970). where c_u is the undrained cohesion of the overconsolidated clay. For piles in sand, as well as in soft clays, k_h can be assumed to linearly vary with depth through a proportionality coefficient n_h, whose values are provided by Poulos and Davis (1980).

Besides determining the behaviour of laterally loaded piles together with their mechanical characteristics and geometry, the coefficients of subgrade reactions influence pile buckling, see for instance Catal and Catal (2006). In this paper, both k_h and the Young's modulus E of the beam were assumed to be constant.

Table 1 Stiffness matrix of a generic i-th element including the contribution of the soil reaction

$\frac{12}{L_i^3}EJ_i+\frac{13}{35}L_ik_i$	$\frac{12}{L_i^3}EJ_i+\frac{13}{35}L_ik_i$	$\frac{12}{L_i^3}EJ_i+\frac{12}{70}L_ik_i$	$\frac{-6}{L_i^2}EJ_i+\frac{13}{420}L_i^2k_i$
….	$\frac{4}{L_i}EJ_i+\frac{1}{105}L_i^3k_i$	$\frac{-6}{L_i^2}EJ_i+\frac{13}{420}L_i^2k_i$	$\frac{2}{L_i}EJ_i-\frac{1}{140}L_i^3k_i$
….	….	$\frac{12}{L_i^3}EJ_i+\frac{13}{35}L_ik_i$	$\frac{-6}{L_i^2}EJ_i-\frac{11}{210}L_ik_i$
….	….	….	$\frac{4}{L_i}EJ_i-\frac{1}{105}L_i^3k_i$

The differential equation of the beam in the Winkler's soil is $k(x)v(x)+M(x)^{II}=0$, where $v(x)$ is the horizontal displacement and $M(x)$ the bending moment. The order of the derivative with respect to the variable x is indicated with a roman numeral superscript, meaning that, for instance, $M(x)^I$ is the shear force $S(x)$. In the following, this notation is adopted,

Both D and the moment of inertia J can be related with A by means of the relations $D=cA^{\beta}$ and $J=hA^{\alpha}$, respectively, where c and h are dimensioned constants and α and β are real numbers. Nondimensional quantities are used, so that nondimensional abscissa ξ, lateral displacement η, cross-sectional area a, diameter d, moment of inertia j, volume v, normal stress ς, coefficient of subgrade reaction χ_{h}, modulus of the top force p_0, shear s and bending moment m are assumed to be, respectively

$$\xi=\frac{x}{l} \qquad \eta=\frac{v}{l} \qquad a=A\frac{l}{V} \qquad d=\frac{d}{l}$$
$$j=\frac{J}{Vl} \qquad v=\frac{V}{l^3} \qquad \varsigma=\sigma\frac{l^{\alpha+2}}{EhV^{\alpha}}$$
$$\chi_h=-k_h\frac{l^{\alpha+5}}{EhV^{\alpha}} \qquad p_0=P_0\frac{l^{\alpha+2}}{EhV^{\alpha}} \tag{2}$$
$$s=S\frac{l^{\alpha+2}}{EhV^{\alpha}} \qquad m=M\frac{l^{\alpha+1}}{EhV^{\alpha}}$$

Therefore, the relations of the nondimensional diameter d and moment of inertia j with a (corresponding to the previously mentioned ones of D and J with A) can be defined as

$$d=\phi a^{\beta} \tag{3}$$

$$j=\psi a^{\alpha} \tag{4}$$

where both $\psi=hV^{\alpha-1}/l^{\alpha+1}$ and $\phi=cV^{\beta}/l^{\beta+1}$are non-dimensional.

3. Distribution of the mass by means of the FSD method

To distribute the mass by means of the FSD method, an iterative algorithm was implemented. At each step, structural analysis was performed by finite elements, so obtaining the bending moment distribution, while the mass distribution was obtained through the FSD method, so obtaining the variation of the cross section along the beam. This causes a variation of the moment distribution, that was then updated through the FE method, thus leading to obtain a new distribution of the cross-section along the beam through the FSD method, until the algorithm converged to the problem solution.

Beam elements with subgrade reaction of the Winkler's medium were used, where the subgrade reaction is dependent on and proportional to the displaced shape of the element. The inverse is also true, that is the displaced shape of the elements depends on the subgrade reaction.

Therefore, if L_i is the length of each i-th element, the following matrix $\mathbf{H}_i$ and its related shape functions $\mathbf{N}_i$ are defined as

$$\mathbf{H}_i=\begin{bmatrix}1 & 0 & 0 & 0\\ 0 & 1 & 0 & 0\\ 1 & L_i & L_i^2 & L_i^3\\ 0 & 1 & 2L_i & 3L_i^2\end{bmatrix} \tag{5}$$

$$\mathbf{N}_i(\xi)=\mathbf{H}_i^{-1^T}\begin{bmatrix}1\\ \xi'\\ \xi'^2\\ \xi'^3\end{bmatrix} \tag{6}$$

where ξ' is the local abscissa. For the principle of virtual works, the stiffness matrix of each i-th element was obtained by integrating the product $\mathbf{N}_i(\xi)^{II}(EJ_i)\,\mathbf{N}_i(\xi)^{II\ T}$ along it.

By algebrically adding the virtual work done by the subgrade to that done by the other applied loads, the stiffness matrix $\mathbf{K}\,s_i$ of each i-th beam element was obtained by adding the matrix $\mathbf{K}_i$ of a beam element not subjected to any subgrade reaction to the matrix $\mathbf{K}\,r_i$ taking into account of the contribution of the subgrade reaction. The matrix $\mathbf{K}\,r_i$ was therefore obtained as the integral of the product $\mathbf{N}_i(\xi)\,(k_{\mathrm{h}}\ D_i)\,\mathbf{N}_i(\xi)^T$ along the element, where $k_i=k_{\mathrm{h}}D_i$ represents the subgrade reaction on each i-th element, see Carrol (1999). The stiffness matrix $\mathbf{K}\,s_i=\mathbf{K}_i+\mathbf{K}\,r_i$ of each element is explicitly shown in Table 1.

After having assembled the global stiffness matrix of the n elements, at each step both displacement v_i and rotation q_i at each node were obtained, as well as the bending moment and its successive derivatives. An iterative algorithm was implemented, where an inner loop distributed the mass of the beam through the FSD method, and updated the moments through FE analysis, while an outer loop optimised the beam length.

The variational method used to obtain the optimum length l is described in the following paragraph, while in this paragraph the application of the FSD method is illustrated by assuming that l is known.

For given nondimensional values m and $\bar{\varsigma}$ of moment and allowable stress $\bar{\sigma}$, respectively, both diameter and cross-sectional area can be obtained from Navier's formula, thus allowing to obtain a fully stressed section. Therefore, by using Navier's formula at any beam section, nondimensional cross-sectional area and diameter were respectively obtained as

$$\mathbf{a} = \left(\frac{1}{2}\frac{\phi}{\psi}\frac{1}{\nu\bar{\varsigma}}m\right)^{\frac{1}{\alpha-\beta}} \tag{7}$$

$$d = \rho\left(\frac{1}{2}\frac{\phi}{\psi}\frac{1}{\nu\bar{\varsigma}}m\right)^{\frac{\beta}{\alpha-\beta}} \tag{8}$$

where, for solid circular cross sections α=2, β=1/2, h=1/(4π), $c=2/\sqrt{\pi}$ and, for circular thin walled hollow sections with wall thickness t, α=3, β=1, $h=1/(8\pi^2t^2)$, $c=1/(\pi t)$.

In general, it is simpler to start from a constant distribution of a and then obtain, by finite elements, the initial distribution of moment $m(\xi)$ from which the first non-constant mass distribution $a(\xi)$ (coinciding with the cross-sectional area distribution for piles with uniform density) is obtained through the FSD method by means of (7). Then, for each successive step of the inner loop, moment and mass distribution are iteratively updated until, for any ξ value, the maximum variation of the mass distribution $\Delta a(\xi)_{max}$ becomes smaller than a given small ε. Therefore, at a generic r-th iteration of the inner loop, the moment is known through a r-th application of the FE method, while the successive (r+1)-th distribution of $a(\xi)$ will be achieved by means of the FSD method. Thus, for each i-th element one obtains:

$$\mathbf{a}_{\mathbf{i}}^{(\mathbf{r+1})} = \left(\frac{1}{2}\frac{\phi}{\psi}\frac{1}{\nu\bar{\varsigma}}m_i^{(r)}\right)^{\frac{1}{\alpha-\beta}} \tag{9}$$

and, at a N-th step, convergence is achieved when, for an assigned sufficiently small positive ε, $|a_i^{(N)}-a_i^{(N-1)}| < \varepsilon$, for i=1, ... n.

Figure 2 shows the nondimensional mass distribution $a(\xi)$ of circular fully stressed beams with solid and hollow thin-walled sections, whose length is also optimised, as shown in the next section.

4. Optimum length

Even if the mass distribution is optimised, a given beam length could be either too short or too long for given total mass. In both cases the beam is not optimised to react to the lateral load, and its top displacement can be minimised through optimising the beam length.

By first reasoning heuristically, if the beam is too short, its length could even tend to zero, with all the mass tending to be close to the beam top, and the beam only slightly embedded in the Winkler's soil, thus becoming ineffective to react to the lateral load. On the contrary, if the beam length tends to be too long, its width tends to become too

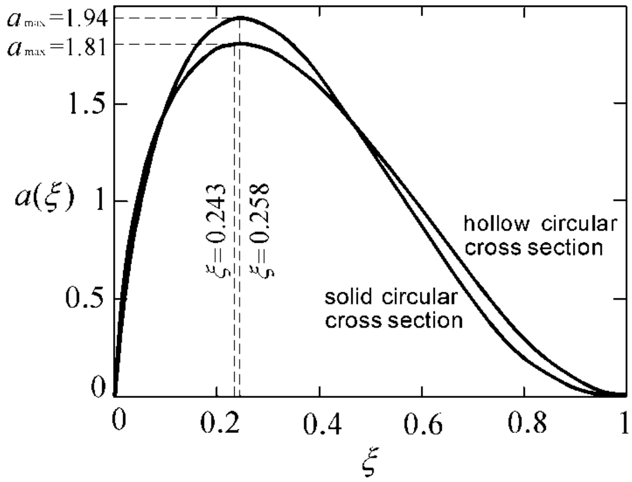

Fig. 2 Distribution of the cross-sectional area $a(x)$ in two different circular beams with optimum length

small (for instance, with length tending to infinity and width tending to zero for given total mass). A too long laterally loaded beam with too small width becomes so slender that moments oscillates between positive and negative values: therefore, when moments are zero, the mass optimization allocates no mass in these points, thus inserting internal hinges along the beam, that it means that such a beam can become more effective to react to the lateral load if its length is decreased. Therefore, together with optimising the mass distribution with the FSD method, the beam length has to be optimised, too, in order to minimise the top displacement.

Optimising the beam length is a variable endpoint problem where, saying l the optimum length, the abscissa $x_l = l$ of the bottom end is unknown. By using variational calculus, the optimum length l can be obtained by imposing a transversality condition at the bottom end (Elsgolts 1980).

Therefore, if F is the integrand function of η_0^*, the transversality condition is

$$[F-(\varphi^I - m^I)dF_{m^{II}}/dx]_{\xi=\xi_l=1} = 0 \tag{10}$$

where $x_l = x_l / l$.

Since the slope of the abscissa axis is zero, then φ^I=0 and, for $x = x_l$=1, we obtain

$$[m^{II}]_{\xi=\xi_l=1} = 0 \tag{11}$$

Thus, l is the abscissa x_l for which m^{II}=0, meaning that there is a flex point at the bottom end, where we also have m^I=m=0.

The flow-chart of Fig. 3 describes the algorithm that optimises the length of the beam by shortening or lengthening it until the transversality condition (11) is satisfied.

Having assigned a length tentative value, in an inner loop the mass distribution is obtained through the FSD method, and, in an outer loop, the optimum length l is obtained by iteratively lengthening or shortening the beam until m^{II}= 0 at the variable endpoint of the bottom end. If

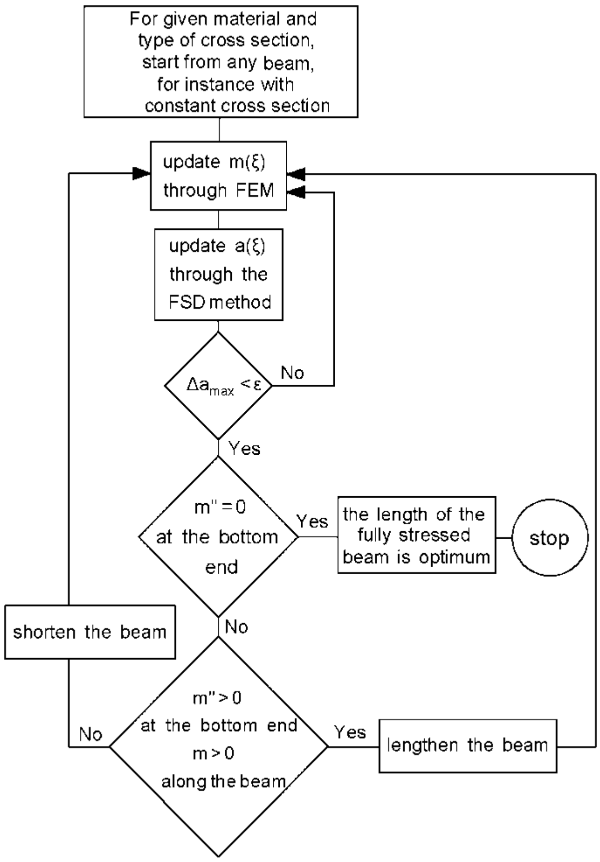

Fig. 3 Numerical algorithm to design fully stressed beams with optimum length

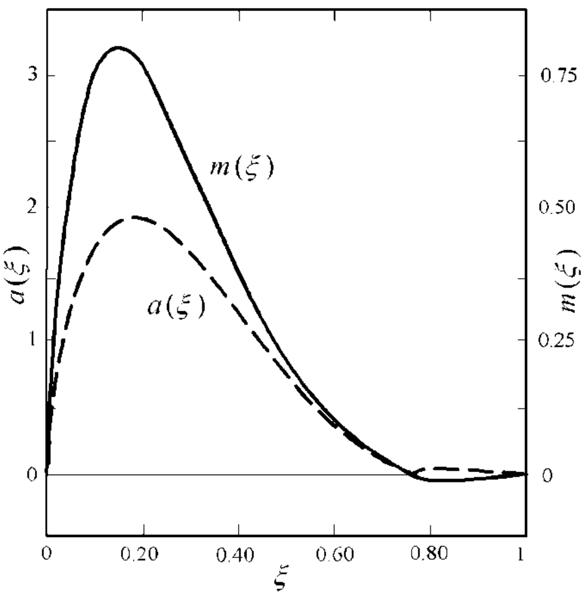

Fig. 4 Hinged solution for fully stressed beams with circular solid cross section and length longer than optimum. This case corresponds, for instance, to a beam 13 m long loaded by P_0=500 kN, and with E=30 GPa, $\bar{\sigma}$ =10 MPa, k_h=20 MPa, V=2.219 m^3

the beam is too short, with also m always positive along the beam and m^{II} positive at the bottom end, the beam is iteratively lengthened until m^{II}= 0.

Contrarily, if the beam is longer than l, the sign of the bending moment changes and m can oscillate several times between positive and negative values, depending on beam and soil stiffness, magnitude of the external load, and beam length. When m changes its sign and becomes zero, for (7) also a becomes zero, meaning that the optimization procedure inserts an internal hinge along the beam (Figure 4). Then, if in the inner loop internal hinges are inserted, in the outer loop the beam is iteratively shortened until m becomes always positive and the transversality condition (11) is satisfied (see Fig. 3).

5. Fully stressed beams with optimum length

Therefore, besides the two cases of too short and too long beams, there is the intermediate one of fully stressed beams with optimum length with m^{II}=0 at the lower end, m>0 along the beam, and m=0 at the ends to meet the boundary conditions.

It can be noted that, for same type of cross section, the mass distributions $a(x)$ of all fully stressed beams with optimum length in a Winkler's medium is always the same, and is therefore a peculiar characteristic of these beams with same type of cross-section. The mass distributions of Fig. 2 are therefore referred to all the circular fully stressed beams with optimum length with solid and hollowthin-walled sections, meaning that $a(x)$ remains unchanged when changing the mechanical properties of the beam material, the coefficient of subgrade reaction of the Winkler's medium, and any constant defining the cross section (i.e. the wall thickness of hollow sections).

Therefore, if the volume V is assigned, the top displacement of fully stressed beams with optimum length results minimised with respect to any fully stressed beam but without optimum length. For beams shorter than l, this minimum results flat. For instance, given the volume V=2.219 m^3, for fully stressed beams with solid circular cross section (E=30 GPa, $\bar{\sigma}$=10 MPa, k_h=20 MPa) loaded by P_0=500 kN, the length decrease from the optimum (l=8.482 m) to the shorter length 6.711 m increases the top displacement v_0 from 26.4 mm to 26.7 mm, that is by only a 1%.

On the contrary, for beams longer than l, the increase of v_0 is higher, because the FSD method inserts inner hinges, thus causing loss of bending stiffness and structural efficiency of the lower part of the embedded beam. For instance, for the beam longer than optimum of Fig. 4 loaded by P_0=500 kN, with same volume 2.219 m^3 but length 13 m, the top displacement is 27.8 mm, that is 5.3% higher than optimum.

It is worth noting that for lengths l_0 longer than l a further optimum exists: in this case, for $0\le x\le l$, the distribution of $A(x)$ is the same of the previous case, while, for $l\le x\le l_0$, $A(x)$ coincides with the abscissa axis, namely $A(x)$ =0. For instance, consider the curve of Fig. 5 and the curve of Fig. 2, both referred to a circular solid section beam. In Fig. 5, the abscissa of all points with $a(x)$>0 and $x<\bar{\xi}=l/l_0=0.8$ is decreased by $(1-\bar{\xi})100$ percent

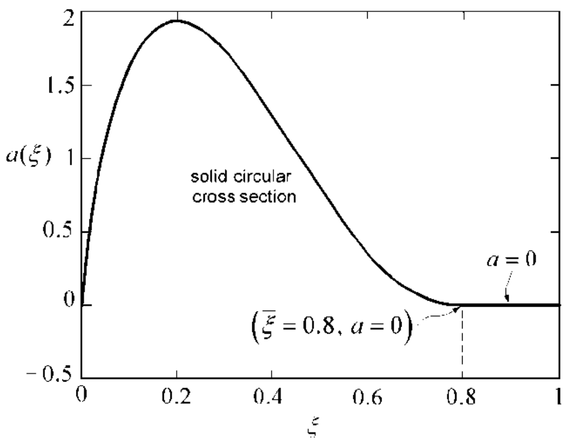

Fig. 5 One-sided variation problem in the lower part of a fully stressed beam

with respect to the abscissa of the corresponding points of a beam with same $a(x)$ obtained through the FSD method but distributed along the optimum length l, as in Fig. 2. hence, apart from the different nondimensional abscissa, for $0 \leq x \leq \bar{\xi}$ the solution of Fig. 5 is identical to that with optimum length l of Fig. 2. Since for $\bar{\xi}$ $x > \bar{\xi}$ both $m(x)$ and $a(x)$ are zero, than for $0 \leq x \leq 1$ (that is $0 \leq x \leq l_0$) there is a point $\bar{\xi} = l/l_0$ where $m^{II}(\bar{\xi})=0$, as well as $m^{I}(\bar{\xi})=m(\bar{\xi})=0$.

This is a one-sided variation problem for both $m(x)$ and $a(x)$ (Myskis 1979), both constrained to coincide with the abscissa axis for $x \geq \bar{\xi}$. The necessary condition $[(\varphi^{I} - m^{I}) dF_m II/dx]_{\xi=\bar{\xi}} = 0$ is then required, that is

$$[m^{I}]_{\xi=\bar{\xi}}\,[m^{II}]_{\xi=\bar{\xi}}\,[m^{III}]_{\xi=\bar{\xi}} = 0 \tag{12}$$

Therefore, either only one of the following three equations is separately satisfied

$$[m^{I}]_{\xi=\bar{\xi}} = 0 \qquad [m^{II}]_{\xi=\bar{\xi}} = 0 \qquad [m^{III}]_{\xi=\bar{\xi}} = 0 \tag{13}$$

or, as it in this case, Eq. (9) are together satisfied, that is

$$[m^{I}]_{\xi=\bar{\xi}} = [m^{II}]_{\xi=\bar{\xi}} = [m^{III}]_{\xi=\bar{\xi}} = 0 \tag{14}$$

This means that, besides the condition (11), optimum beams with optimum length require the further condition $m^{III}=0$ at the bottom end. Fig. 5 shows that, at the point with abscissa $\bar{\xi}$ along the abscissa axis, Eq. (14) are satisfied for both the left derivatives (on the side with $a(x)>0$, $m(x)>0$), and the right derivatives (where $m(x)=a(x)=0$, thus coinciding with the abscissa axis). Therefore, at this point with abscissa $\bar{\xi}$, Weierstrass-Erdmann conditions are satisfied, meaning that m and a are free from break-points and smoothly merge with the abscissa axis (Banichuk and Karihaloo 1977).

6. Examples

Consider for instance the case of a fully stressed beam with optimum length with solid circular cross-section. This type of cross-section, whose nondimensional mass distribution $a(x)$ is shown in Fig. 2, is characterized by $h=1/(4\pi)$ and $c=2/\sqrt{\pi}$ (see Section 3).

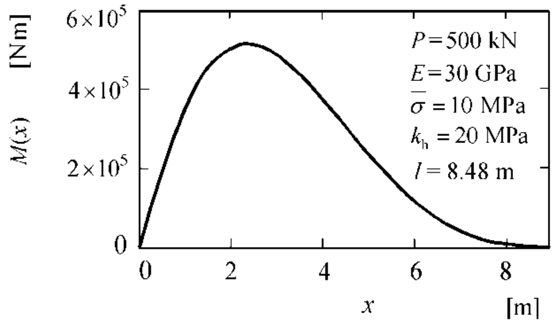

Fig. 6 Bending moment in a fully stressed beam with optimum length with circular solid cross-section. Material properties and external load are indicated in the legend

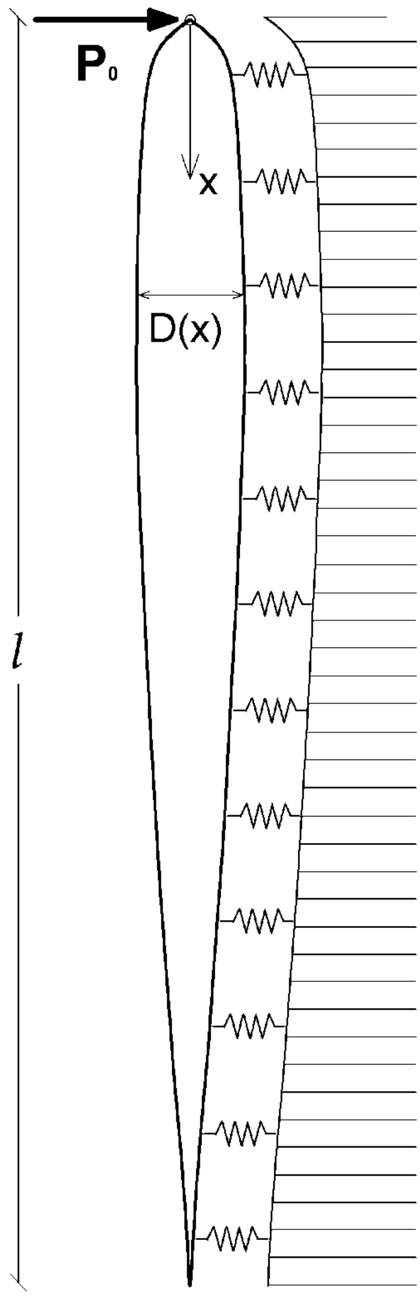

Fig. 7 Shape of the fully stressed beam with optimum length whose mechanical characteristics are shown in Fig. 6

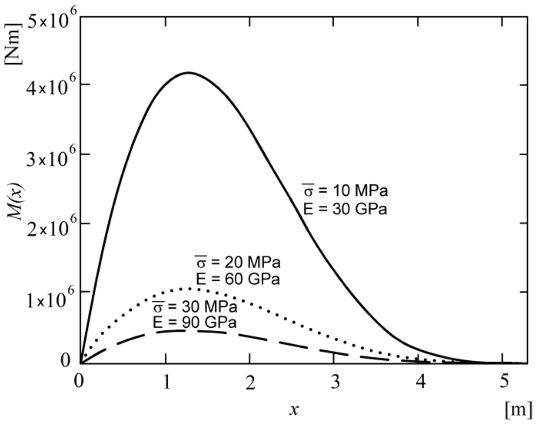

Fig. 8 Moment distribution in hollow section piles subjected to the same lateral load of 500 kN and made of concrete with different material characteristics

The lateral load at the top is P_0=500 kN. Elastic modulus and allowable stress of the beam material are E=30 GPa and $\bar{\sigma}$ =10 MPa, respectively; the coefficient of subgrade reaction is k_h=20 MPa/mm. Using the algorithm described in Fig. 3, functions $m(\xi)$ and $a(\xi)$ are drawn and, for $m^I|_{\xi=1}=m^{II}|_{\xi=1}=0$, the optimum length l=8.481 m with volume V=2.219 m^3 is also obtained (with $\bar{\varsigma}$=316.63 and χ_h=5372, v=3.637·10^{-3}, ϕ=0.0681 and ψ=2.894·10^{-4}).

The nondimensional lateral force applied at the top, coinciding with the first derivative $dm/d\xi|_{\xi=0}$ at the top boundary, is therefore $p_0=P_0\, l^{\alpha+2}/(EhV^{\alpha})$=0.22.

The moment distribution $M(x)$ along the beam is then obtained (see Fig. 6), together with the mass distribution $A(x)$ that allows to obtain the shape of the laterally loaded pile under consideration (Fig. 7). This example can be referred to an optimised laterally loaded pile made of reinforced concrete, and embedded in an overconsolidated cohesive soil with undrained cohesion c_u=0.30 MPa, with $k_h \cong 67\, c_u$/mm = 20.1 MPa/mm [1].

A laterally loaded pile made of reinforced concrete with solid circular cross section and with optimum shape and length could be constructed by first prefabbricating a hollow section pile with same shape made of centrifuged concrete, and, after embedding the pile into the soil, by then pouring the fluide concrete into the hollow-section pile, thus obtaining a solid cross-section pile. The procedure of filling with concrete a hollow section pile after embedding it is used in “Multiton” piles (Fenu 2006), where steel tubes with diameter decreasing with depth are first embedded into the soil and then filled with concrete to increase their load bearing capacity.

On the contrary, if hollow-section piles are chosen (that are much lighter than the solid-section ones, depending on the wall thickness), there is no need to fill them with concrete, because their shape is optimised to maximize their performance.

Consider therefore a hollow-section pile laterally loaded at the top by the same force P_0=500 kN, embedded in the same above soil with coefficient of subgrade reaction k_h=20 MPa/mm. Since to prefabricate a hollow-section pile, centrifuged concrete reinforced by steel meshes can be used, concrete with higher mechanical properties is considered, for instance with E=90 GPa and $\bar{\sigma}$=30 MPa.

Using the same procedure described in Fig. 3, the optimum length l=5.292 m and the volume V=0.246437 m^3 are obtained (with ς=511.033, χ_h=1803, v=1.663·10^3, ϕ=0.0560 and ψ=3.923·10^{-4}).

The moment distribution $M(x)$ along the beam (Fig. 8) is then drawn, together with the mass distribution $A(x)$, that leads to the shape of the hollow-section pile under consideration shown in Figure 9a, with maximum diameter D_{max} = 0.585 m.

If a concrete with lower mechanical properties is used (E=60 GPa and $\bar{\sigma}$=20 MPa), the optimum length does not change, but the pile volume is increased to V=0.301823 m^3 (with $\bar{\varsigma}$ =278.17, χ_h=1472, v=2.036·10^{-3}, ϕ=0.0686 and ψ=5.884·10^{-4}). Fig. 8 shows that the moment level becomes much higher (M_{max} about 2 times higher), while Fig. 9(b) shows the related pile shape with increased diameters (D_{max} = 0.705 m). By further decreasing elastic modulus and allowable stress (E=30 GPa and $\bar{\sigma}$=10 MPa), the optimum length is still the same, but the volume of the pile is to be increased to V=0.426842 m^3(with $\bar{\varsigma}$=98.348, χ_h=1041, v=2.880·10^{-3}, ϕ=0.0970 and ψ=1.177·10^{-3}). The related moment distribution $M(x)$ of Figure 8 shows that the moment level becomes much higher (M_{max} about 4 times higher than in the previous case), while a stocky pile is obtained (Fig. 9(c)) with maximum diameter further increased to almost 1 m (namely 0.976 m). Therefore, by shaping optimum hollow-section piles laterally loaded at the top, if high performance concrete is not used, too stocky piles are obtained.

A further example with different materials is also presented. Consider a dowel fastener made of steel embedded in wood. Since in this case a circular solid cross section is used, the nondimensional mass distribution $a(\xi)$ is the same of the pile with solid circular section considered above (see Fig. 1). By assuming k_h=10500 MPa, E=205 GPa, and $\bar{\sigma}$=300 MPa, if the orthogonal load on the fastener is P_0 = 3 kN, the optimum length is l=117 mm with V=6000 mm^3 (and with $\bar{\varsigma}$ =1290.730, χ_h=5366, v=3.775·10^{-3}, ϕ=0.0693 and ψ=3.004·10^{-4}). The maximum diameter is D_{max}= 11.2 mm.

7. Conclusions

The optimised design of laterally loaded beams in a Winkler’s medium can be iteratively obtained through the Fully Stressed Design method, a simple optimality criterion that has shown to be effective for this aim.

Structural analysis of the beam with variable cross-sectional-area has been carried out by finite elements (thus determining bending moments), while the cross-sectional area has been contemporarily updated through the FSD method until achieving convergence.

A simple method of optimising the length of optimum beams has been defined by using variational calculus. Therefore, while in an inner loop the optimum mass distribution is obtained, in an outer loop the beam length is

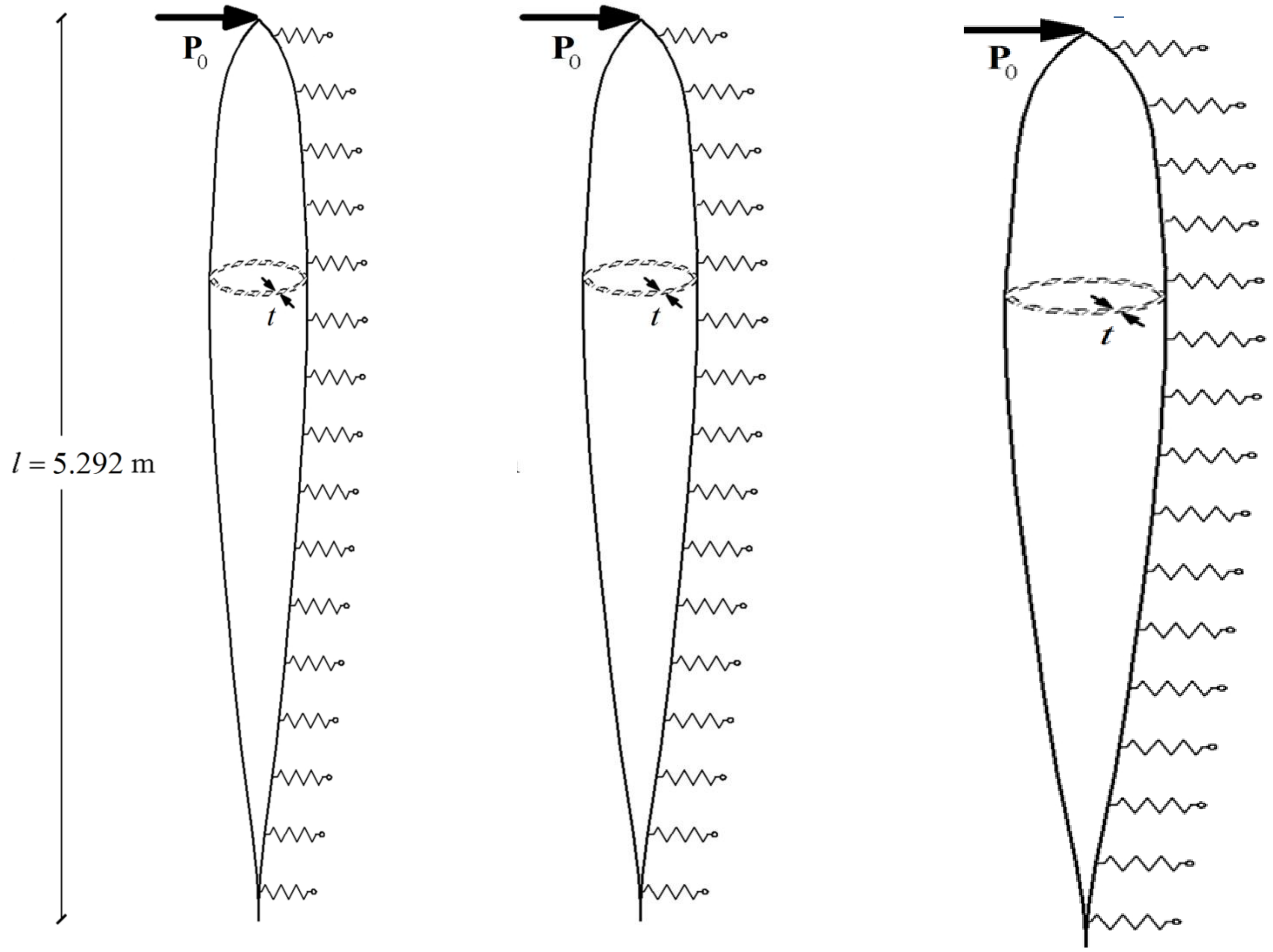

(a) (b) (c)

Fig. 9 Shape of hollow section piles made of concrete with different mechanical characteristics. (a) E=90 GPa, $\bar{\sigma}$=30 MPa; (b) E=60 GPa, $\bar{\sigma}$=20 MPa; (c) E=30 GPa, $\bar{\sigma}$=10 MPa

increased or decreased until the necessary condition defined through variational calculus to obtain the optimum beam length is met.

The method has shown to be robust and efficient because the FSD method does not require any derivative to find the optimum mass distribution, while the necessary condition that must be satisfied to find the optimum length requires to calculate the second derivative only at the beam bottom end.

Some examples referred to different fields are reported. In fact, both steel fasteners embedded in wood and laterally loaded piles embedded in soil can be considered as laterally loaded beams surrounded by a Winkler's medium. For the mass production of steel fasteners can be useful to optimise both their length and their mass distribution, depending on the service conditions. Additionally, some examples show that in Geotechnics laterally loaded piles with optimum mass distribution and length could be prefabricated with hollow sections. In this case, centrifuged concrete with high mechanical properties reinforced with steel meshes can be used. Optimum laterally loaded piles made of concrete with high characteristics have shown to have much lower moments and smaller cross-sections with respect to piles made of normal concrete.

Normal concrete can be instead used for optimum laterally loaded piles with solid cross-section. In this case the pile should be still constructed with centrifuged concrete with hollow section, but suitably shaped to work with solid section, that can be obtained by pouring fluid concrete into the hollow section pile after embedding it. .

Acknowledgments

The research was supported by the FIR fund of the University of Cagliari (Cagliari, Italy), and by the Recruitment Program of Global Experts Foundation (Grant No. TM2012-27), National Natural Science Foundation of China (Grant No. 51778148). The authors would also like to acknowledge the Sustainable and Innovative Bridge Engineering Research Center (SIBERC) of the College of Civil Engineering, Fuzhou University (Fuzhou, China), and the Department of Civil Engineering, Environmental Engineering and Architecture of the University of Cagliari.

References

Poulos, H.G. and Davis, E.H. (1980), *Pile Foundation Analysis and Design*, John Wiley & Sons, Inc., New York, U.S.A.

Bowles, J.E. (1996), *Foundation Analysis and Design*, McGraw-Hill, 5th edition, New York, U.S.A.

Haftka, R.T. and Gürdal, Z. (1993), *Elements of Structural Optimization*, Kluwer Academic Publishers, Dordrecht, Boston, London.

Fenu, L. and Serra, M. (1995), "Optimum design of beams surrounded by a Winkler's medium", *Struct. Opt.*, **9**, 132-135.

Fenu, L. (2005), "On the characteristics of optimum beams with optimum length surrounded by a Winkler's medium", *Struct. Mult. Opt.*, **30** (3), 243-250.

Fenu, L. and Madama, G. (2006) "Laterally loaded R/C bored piles with minimum horizontal top displacement", *Proceedings of the 2nd fib Congress*, Naples, Italy, June.

Lan, C., Briseghella, B., Fenu, L., Xue, J. and Zordan, T. (2017), "Piles optimal shapes in integral abutment bridges", *J. Traff. Transp. Eng.*, **4**(6), 576-593.

Zordan, T. and Briseghella, B. (2007), "Attainment of an integral abutment bridge through the refurbishment of a simply supported structure", *Struct. Eng. Int.* (SEI), **17**(3), 228-234.

Briseghella, B. and Zordan T. (2007), "Integral abutment bridge concept applied to the rehabilitation of a simply supported concrete structure", *Struct. Concrete*, **8**(1), 25-33.

Zordan, T., Briseghella, B. and Lan, C. (2011), "Parametric and pushover analyses on integral abutment bridge", *Eng. Struct.*, **33**(2), 502-515.

Zordan, T., Briseghella, B. and Lan C. (2011), "Analytical formulation for limit length of integral abutment bridges", *Struct. Eng. Int.* (SEI), **21**(3), 304-310.

Kim, W. and Laman, J.A. (2013), "Integral abutment bridge behavior under uncertain thermal and time-dependent load", *Struct. Eng. Mech.*, **46**(1), 53-73.

Kim, W., Laman, J.A. and Park, J.Y. (2014), "Reliability-based design of prestressed concrete girders in integral Abutment Bridges for thermal effects", *Struct. Eng. Mech.*, **50**(3), 305-322

Far, N.E., Maleki, S. and Barghian, M. (2015), "Design of integral abutment bridges for combined thermal and seismic loads", *Earthq. Struct.*, **9**(2), 415-430.

Nakhaee, M. and Johari, A. (2013), "Genetic based modelling of undrained lateral load capacity of piles in cohesion soils", *Glob. J. Sci. Eng. Technol.*, **5**, 123-133.

Eicher, J.A., Guan, H. and Jeng, D.S. (2002), "A parametric study of a offshore concrete pile under combined loading conditions using finite element method", *Electr. J. Struct. Eng.*, 1.

Baki, S.A., Al-Jassim, J. and Qasim, R.M. (2016), "Parametric study of the lateral behavior of cast in drilled hole piles", *Am. J. Civil Eng.*, **4**(5), 247-253.

Mehndirattaa, S., Sawant, V.A. and Samadhiya, N.K. (2014), "Nonlinear dynamic analysis of laterally loaded pile", *Struct. Eng. Mech.*, **49**(4), 479-489.

Gandomi, A.H. and Alavi, A.H. (2012), "A new multi-gene genetic programming approach to non-linear system modelling. Part II: Geotechnical and earthquake engineering problems", *Neur. Comput. Appl.*, **21**, 189-201.

Imancli, G., Kahyaoglu, M.R., Ozden, G. and Kayalar, A.S. (2009), "Performance functions for laterally loaded single concrete piles in homogeneous clays", *Struct. Eng. Mech.*, **33**(4), 529-537.

Winkler E. (1867), *Die Lehre von der Elastizität und Festigkeit*, Verlag Dominicus, Prague, Czech Republic.

Baguelin, F., Frank, R. and Said, Y.H. (1997), "Theoretical study of lateral reaction mechanism of piles", *Geotech* Prague, **27**(3), 405-434.

David, T.K. and Forth, J.P. (2011), *Modelling of Soil Structure Interaction of Integral Abutment Bridges*, World Academy of Science, Engineering and Technology, 5, 2011-06-26, 645-650.

Ashour, M. and Norris, G. (2000), "Modelling lateral soil-pile response based on soil-pile interaction", *J. Geotech. Geoenviron. Eng.*, **126**(5), 420-428.

Boulanger, R.W., Curras, C.J., Kutter, B.L., Wilson, D.W. and Abghari, A. (1999), "Seismic soil-pile-structure interaction experiments and analyses", *J. Geotech. Geoenviron. Eng.*, **125**(9), 750-759.

Kim, Y. and Jeong, S. (2011), "Analysis of soil resistance on laterally loaded piles based on 3d soil-pile interaction", *Comp. Geotech.*, **2**, 248-257.

Kavitha, P.E., Beena, K.S. and Narayanan, K.P. (2016), "A review on soil-structure interaction analysis of laterally loaded piles", *Innov. Infrastruct. Solut.*, **1**, 14.

McGann, C.R. and Arduino, P. (2011), *Laterally-Loaded Pile Foundation*, from OpenSeesWiki: <http://opensees.berkeley.edu/wiki/index.php/Laterally-Loaded_Pile_Foundation>.

McGann, C.R., Arduino, P. and Mackenzie-Helnwein, P. (2011), "Applicability of conventional p-y relations to the analysis of piles in laterally spreading soil", *J. Geotech. Geoenviron. Eng.*, **137**(6), 557-567.

Chik, K.H., Abbas, J.M. and Taha, M.R. (2008), "Single pile simulation and analysis subjected to lateral load", *EJGE-Electr. J. Geotech. Eng.*, 13.

Ahmadi, M.M. and Ahmari, S. (2009), "finite element modelling of laterally loaded piles in clay", *Proceedings of the Institution of Civil Engineering-Geotechnical Engineering*, **162**(3), 151-163.

Juirnarongrit, T. and Ashford, S.A. (2004), "Lateral load behaviour of cast-in-drilled-hole piles in weakly cemented sand", *Transp. Res. Rec. J. Transp. Res. Board*, **1868**, 190-198.

Broms, B.B. (1964), "Lateral resistance of piles in cohesive soils", *J. Soil Mech. Found. Div.*, **90**(2), 27-64.

Broms, B.B. (1964), "Lateral resistance of piles in cohesion less soils", *J. Soil Mech. Found. Div.*, **90**(3), 123-158.

Kok, S.T. and Huat B.B.K. (2008) "Numerical modelling of laterally loaded piles", *Am. J. Appl. Sci.*, **5**(10), 1403-1408.

Krishnamoorthy, N. and Sharma, K.J. (2008), "Analysis of single and group of piles subjected to lateral load using finite element method", *Proceedings of the 12th International Conference of International Association for Computer Methods and Advances in Geomechanics (IACMAG) Goa*, India, October.

Phanikanth, V.S., Choudhury, D. and Rami Reddy, G. (2010), "Response of single pile under lateral loads in cohesion less soils", *EJGE-Electr. J. Geotech. Eng.*, 15.

Wakai, A., Gose, S. and Ugai, K. (1999), "3D Elasto-plastic finite element analyses of pile foundations subjected to lateral loading", *Soil. Foundat. (The Jap. Geotech. Soc.)*, **39**(1), 97-111.

Yang, Z. and Jeremic, B. (2002), "Numerical analysis of pile behaviour under lateral loads in layered elastic-plastic soils", *Int. J. Numer. Analy. Meth. Geo Mech.*, **2**, 1-31.

Reese, L.C. and Desai, C.S. (1977), *Laterally Loaded Piles*, In: Desai, C.S. and Christian, J.T. (Edited by) *Numerical Methods in Geotechnical Engineering*, McGraw-Hill Book Company, New York, U.S.A.

Brown, D.A. and Shie, C.F. (1990), "Three dimensional finite element model of laterally loaded piles", *Comp. Geotech.*, **10**(1), 59-79.

Han, J. and Frost, J.D. (2000), "Load-deflection response of transversely isotropic piles under lateral loads", *Int. J. Numer. Anal. Meth. Geomech.*, **24**(5), 509-529.

Bartholomew, P. and Morris, A.J. (1976), "A unified approach to fully-stressed design", *Eng. Opt.*, **2**(1), 3-15.

Patnaik, S.N. and Hopkins, D.A. (1998), "Optimality of a fully stressed design", *Comp. Meth. Appl. Mech. Eng.*, **165**(1-4),215-

221.
Briseghella B., Fenu, L., Feng, Y., Lan, C., Mazzarolo, E. and Zordan, T. (2016), "Optimization indexes to identify the optimal design solution", *J. Brid. Eng.*, **21**(3), 04015067-1-04015067-12.
Briseghella, B., Fenu, L., Feng, Y., Mazzarolo, E. and Zordan, T. (2013), "Topology optimization of bridges supported by a concrete shell", *Struct. Eng. Int.*, **23**(3), 285-294.
Briseghella, B., Fenu, L., Lan, C., Mazzarolo, E. and Zordan, T. (2013), "Application of topological optimization to bridge design", *J. Brid. Eng.*
Fiore, A., Marano, G.C., Greco, R. and Mastromarino, E. (2016), "Structural optimization of hollow-section steel trusses by differential evolution algorithm", *Int. J. Steel Struct.*, **16**(2) 411-423.
Greco, R., Marano, G.C. and Fiore, A. (2016), "Performance-cost optimization of tuned mass damper under low-moderate seismic actions", *Struct. Des. Tall Spec. Build.*, **25**(18) 1103-1122.
Greco, R. and Marano, G.C. (2016), "Robust optimization of base isolation devices under uncertain parameters", *JVC/J. Vibr. Contr.*, **22**(3), 853-868.
Lucchini, A., Greco, R., Marano, G.C. and Monti, G. (2014), "Robust design of tuned mass damper systems for seismic protection of multistory buildings", *J. Struct. Eng.*, **140**(8), A4014009.
Marano, G.C., Trentadue, F. and Petrone, F. (2014), "Optimal arch shape solution under static vertical loads", *Acta Mech.*, **225**(3) 679-686.
Marano, G.C. and Greco, R. (2011), "Optimization criteria for tuned mass dampers for structural vibration control under stochastic excitation", *JVC/J. Vibr. Contr.*, **17**(5), 679-688.
Marano, G.C., Greco, R., Quaranta, G., Fiore, A., Avakian, J. and Cascella, D. (2013), "Parametric identification of nonlinear devices for seismic protection using soft computing techniques", *Adv. Mater. Res.*, **639-640**(1) 118-129.
Quaranta, G., Fiore, A. and Marano, G.C. (2014), "Optimum design of prestressed concrete beams using constrained differential evolution algorithm", *Struct. Mult. Opt.*, **49**(3), 441-453.
Zordan, T., Briseghella, B. and Mazzarolo, E. (2010), "Bridge structural optimization through step-by-step evolutionary process", *Struct. Eng. Int.* (SEI), **20**(1), 72-78.
Palmer, L.A. and Thompson, J.B. (1948), "The earth pressure and deflection along the embedded lengths of piles subjected to lateral thrusts", *Proceedings of the 2nd International Conference on Soil Mechanics and Foundation Engineering*, Rotterdam, the Netherlands. June.
Davisson, M.T. (1970), *Lateral Load Capacity of Piles*, Highway Research Record, NO.333, Washington, D.C., U.S.A., 104-112.
Catal, S. and Catal, H.H. (2006), "Buckling analysis of partially embedded pile in elastic soil using differential transform method", *Struct. Eng. Mech.*, **24**, 247-268
Carrol, W.F. (1999), *A Primer for Finite Elements in Elastic Structures*, John Wiley & Sons, Inc., New York, U.S.A.
Elsgolts, L.E. (1980), *Differential Equations and the Calculus of Variations*, English Edition, MIR Publishers, Moscow, USSR.
Myskis, A.D. (1979), *Advanced Mathematics for Engineers*, English Edition, MIR Publishers, Moscow, USSR.
Banichuk, N.V. and Karihaloo, B.L. (1977), "On the solution of optimization problems with singularities", *Int. J. Sol. Struct.*, **13**(8) 725-733.
Fenu, L. (2006), "Pali multiton caricati lateralmente e con spostamento minimo", *Proceedings of the 16th CTE Conference*, Parma, Italy, November.

CC